J Mater Sci (2008) 43:2276–2285
DOI 10.1007/s10853-007-2023-x

Morphology and structure of rare earth borate ($REBO_3$) synthesized by glycothermal reaction

Saburo Hosokawa · Yusuke Tanaka · Shinji Iwamoto · Masashi Inoue

Received: 6 November 2006 / Accepted: 20 July 2007 / Published online: 29 November 2007

Abstract The glycothermal reaction of the rare earth (RE) acetates with trimethoxyborane (RE/B = 1) at 315 °C for 2 h yielded $REBO_3$ for Tm, Yb and Y. For Gd–Er, $REBO_3$ was contaminated with amorphous products. Mixtures of RE(OAc)O, $REBO_3$ and amorphous products were obtained for Sm and Eu, while only $RE(OAc)_2(OH)$ was obtained for La. The space group of the $REBO_3$ crystal obtained from Sm–Er and Y was $P6_3/m$, and mixture of $REBO_3$ crystals with $P6_3/m$ and $R\bar{3}c$ were obtained for Tm and Yb. Prolonged reaction time (6 h) yielded $REBO_3$ without contamination of the amorphous product or RE(OAc)O for Eu–Yb and Y. For the reaction of yttrium acetate and trimethoxyborane with Y/B ratio of 1/3–3/1 for 2 h, YBO_3 was only the binary oxide detected. The YBO_3 particles were spheroidal with a diameter of 1 μm. The selected area electron diffraction of a whole particle indicated that the each particle is a "single crystal" of YBO_3 grown from one nucleus.

Introduction

A large number of luminescent materials based on rare earth (RE) ions or RE host lattices has been developed [1]. RE borates with the vaterite structure, in particular $(Gd,Y)BO_3$:Eu, represent an important material for plasma display panels. The luminescent property of phosphor materials is strongly affected by the particle size and morphology. Surface perfect and spherical-shaped phosphor always has high packing density, good slurry property, and smoother light intensity distribution [2].

Various techniques have been developed to prepare high-quality $REBO_3$:Eu phosphors, such as solid-state reaction [3], coprecipitation method [3, 4], combustion synthesis [5], ultrasonic spray pyrolysis [6], sol-gel technique [7, 8] and sol-gel pyrolysis process [9, 10]. A number of works have been devoted on hydrothermal synthesis of $REBO_3$, and $REBO_3$ nanoparticles or $REBO_3$ with specific morphologies were obtained by this method [2, 11–15]. For example, Yan et al. prepared YBO_3:Eu nanoparticles (particle size; 20 nm) by a hydrothermal method in the presence of urea [13]. They also have reported the formation of donut-like assembly of YBO_3:Eu crystals by the hydrothermal method under an alkaline condition [14]. Lin et al. have reported that YBO_3:Eu crystals with flower-and hedgehog fungus-like structures were synthesized by the hydrothermal method under acidic conditions [15].

We have been exploring the synthesis of inorganic materials in organic media at elevated temperatures (200–300 °C) under the autogenous pressure of the media. Various mixed oxides were directly crystallized under mild conditions when two suitable starting materials such as alkoxide, acetylacetonate, or acetate were allowed to react in 1,4-butanediol at 200–300 °C [16–18]. This reaction procedure using glycol as the organic solvent was termed "glycothermal," since the use of glycol in place of water for hydrothermal reaction.

In the present work, the morphology and structure of $REBO_3$ obtained by the glycothermal reaction of RE acetates with trimethoxyborane in 1,4-butanediol are investigated.

S. Hosokawa · Y. Tanaka · S. Iwamoto · M. Inoue (✉)
Department of Energy and Hydrocarbon Chemistry, Graduate School of Engineering, Kyoto University, Katsura, Kyoto 615-8510, Japan
e-mail: inoue@scl.kyoto-u.ac.jp

Experimental

Trimethoxyborane (1.29 g, 12.5 mmol) and yttrium acetate tetrahydrate (4.24 g, 12.5 mmol) were suspended in 120 mL of 1,4-butanediol (1,4-BG) in a test tube, serving as autoclave linear, and the test tube was placed in a 300 mL autoclave. An additional 40 mL of 1,4-BG was placed in the gap between the autoclave wall and the test tube. The autoclave was purged with nitrogen, heated to 315 °C at a rate of 2.3 °C/min, and kept at that temperature for 2 h. After the assembly was cooled to room temperature, the resulting products were centrifuged. The product was washed with methanol by vigorous mixing and centrifuging and then air-dried. For calcination, the products were heated at a rate of 10 °C/min and held at a prescribed temperature for 30 min in a box furnace.

X-ray powder diffraction (XRD: Model XD-D1 Shimadzu, Kyoto, Japan) was recorded using Cu $K\alpha$ radiation. For Rietveld analysis, the XRD pattern was measured on another diffractometer (Model Rint 2500, Rigaku, Tokyo, Japan) and analyzed by RIETAN-2000 program [19]. The morphology of the products was observed with a scanning electron microscope (SEM), Hitachi S-2500CX, and a transmission electron microscope (TEM), Hitachi H-800. Specific surface area was calculated using the BET single-point method on the basis of N_2 uptake measured at 77 K using a Micrometritics Flowsorb II 2300 sorptionmeter. Nitrogen adsorption isotherm was measured using a volumetric gas-sorption system (Model Autosorb-1, Quantachrome, USA). Simultaneous thermogravimetric and differential thermal analyses were performed on a thermal analyzer (Model DTG-50, Shimadzu, Kyoto, Japan) at a rate of 5 °C/min in a 40 mL/min flow of dried air. The particle size distribution was measured on an electrophoretic light scattering spectrometer, Otsuka Electronics, ELS-800. A portion of the product (25 mg) was suspended in 250 mL of distilled water. The measurement was carried out after ultrasonic treatment of the suspension for 10 min, followed by standing for 10 min.

Results and discussion

Synthesis of YBO_3 by the glycothermal reaction

Figure 1 shows the XRD patterns of the as-synthesized products obtained by the reaction with various ratios of yttrium acetate to trimethoxyborane at 315 °C for 2 h. A clear solution was obtained by the reaction of trimethoxyborane alone. YBO_3 was obtained by the reaction of Y/B = 1 and 1/3. Y(OAc)O was formed in the product with Y/B = 3/1, but the phase due to boron species was not detected [20]. The amount of the product obtained

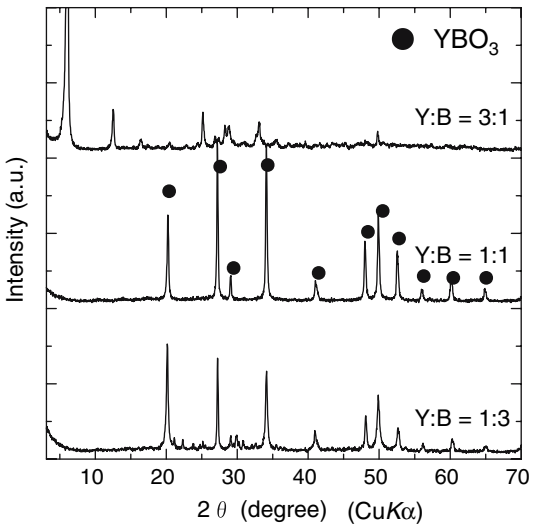

Fig. 1 XRD patterns of the products as synthesized by the glycothermal reaction of yttrium acetates and trimethoxyborane with various ratios in 1,4-BG at 315 °C for 2 h

by Y/B = 1 was ca. 1.8 g, and the ceramic yield calculated on the basis of the observed weight loss of the product yielding YBO_3 by calcination at 1,000 °C was above 90%. However, the yield was low for the reaction with Y/B of 1/3. Another yttrium borate phase, Y_3BO_6, has been reported [21, 22], but only YBO_3 was obtained in the glycothermal reaction of yttrium acetate and trimethoxyborane.

Figure 2 and Table 1 show the results for Rietveld analysis of the YBO_3 product as synthesized by the reaction of yttrium acetate and trimethoxyborane with Y/B = 1. The refinement led to residual values of $R_{wp} = 7.45\%$, $R_p = 5.46\%$, $R_e = 2.97\%$ and $S = 2.51$. The space group of YBO_3 was $P6_3/m$ [23]. The unit cell parameters for a and c axes were 3.796 ± 0.002 and 8.815 ± 0.003 Å, respectively, which were slightly larger than the reported values (a, 3.776 Å; b, 8.806 Å) [23]. Enlargement of the unit cell is usually observed for the glycothermal products and is attributed to the alkoxyl (or hydroxyl) groups anchored on the surface of the product particles.

The as-synthesized YBO_3 was composed of spheroidal particles with hexagonal-pyramidal craters at the both sides of the particles (Fig. 3a). The largest diameter was 1 μm, which was distributed in a extremely narrow range, and agglomerates were not observed, indicating mono-dispersed particles were formed. The particle size distribution was also assessed by the dynamic light scattering method (Fig. 4). The particle size was distributed in a range of 0.4–1.0 μm, slightly smaller than that observed by SEM, which is, however, reasonable because the product particles were not truly spherical. The distribution curve also indicates that the product particles were well dispersed and free from agglomerates.

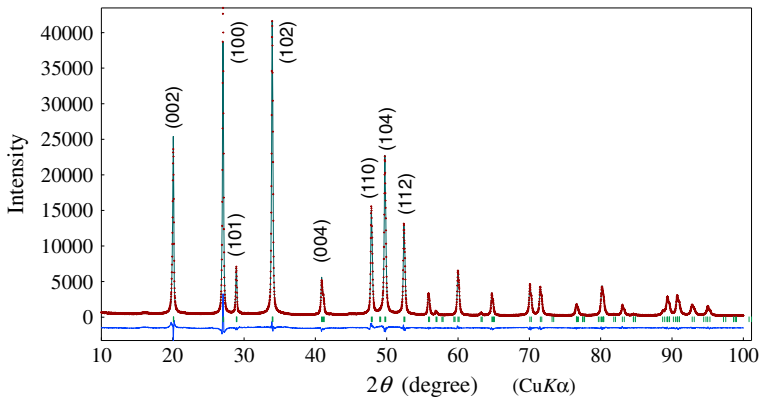

Fig. 2 Observed, calculated, and difference patterns obtained by Rietveld analysis of YBO_3 as synthesized by glycothermal reaction at 315 °C for 2 h

Table 1 Crystallographic data of YBO_3 obtained by glycothermal method

Element	Site	g[a]	Atomic coordinates			B[b]
			x	y	z	
Oa	4*f*	1	0.667	0.333	0.105 ± 0.0003 (0.1103)[c]	1.0 (1.5)
Ob	6*h*	1/3	0.783 ± 0.001 (0.774)	−0.132 ± 0.007 (−0.119)	0.250	1.0 (0.5)
B	6*h*	1/3	0.593 ± 0.015 (0.586)	0.438 ± 0.014 (0.435)	0.250	1.0 (0.4)
Y	2*b*	1	0	0	0	0.5 (0.273)

Space group $P6_3/m$ (No. 176)

[a] Site occupacy

[b] Isotropic displacement parameter

[c] The value was reported by reference [23]

The TEM images of the as-synthesized YBO_3 particles are shown in Fig. 5. As shown in Fig. 5a, crushed particles were frequently observed. All of them appeared to be originated from the spheroidal particles, which were crushed through the center of the spheroid during the preparation of the specimens for TEM observation. Detailed examination of the TEM images of the crushed particles indicated that the particles contained a number of deep crevices, which can explain the reason why the spheroidal particles are easily broken down. The selected area electron diffraction of a whole particle exhibited a single crystal pattern with the *c* axis of the YBO_3 crystal parallel to the electron beam (Fig. 5b). These results suggest that each particle was grown from one nucleus, but was divided into smaller crystallites by the crevices. Figure 5c shows a high magnification image of the edge of the YBO_3 crystals whose *ab* planes are parallel to the electron beam. Thin plates of the YBO_3 crystals were preferentially grown along with the *ab* plane. However, the plates were not stacked in parallel but with slight angles, resulting in formation of the spheroidal particles with the craters at the both sides as shown in the SEM image. Detailed mechanisms for the formation of the unique morphology of the product particles will be discussed in a separate paper.

Differential thermal analysis (DTA) of the as-synthesized YBO_3 product obtained by the reaction at 315 °C showed a slight exotherm at around 350 °C, which was associated with about 2.0% weight decrease between 200 and 400 °C (Fig. 6). This weight decrease is due to the combustion of the organic residue remaining on the product particles. No sharp peak due to the crystallization of the amorphous phase was observed in DTA up to 1,200 °C, but a weight loss was detected between 1,100 and 1,200 °C. The XRD patterns of the samples obtained by calcination at 500 and 800 °C were essentially identical with that of the as-synthesized product (Fig. 7). However, the XRD pattern of the product calcined at 1,100 °C exhibited low intensity peaks at 22.0, 32.8 and 31.1°, which are presumably due to Y_3BO_6 [21, 22]. This result indicates that segregation of YBO_3 into Y_3BO_6 and B_2O_3 occurred followed by evaporation of B_2O_3 since boron oxide is known as a highly volatile material with the boiling point of 1,800 °C and the vapor pressure of 1.16×10^{-6} Pa at 800 °C [24]. The calcined products were well dispersed and sintering of the particles (1 μm) were not observed in the SEM images (Fig. 3b, c).

Some properties of the as-synthesized YBO_3 and the samples obtained by calcination thereof are summarized in

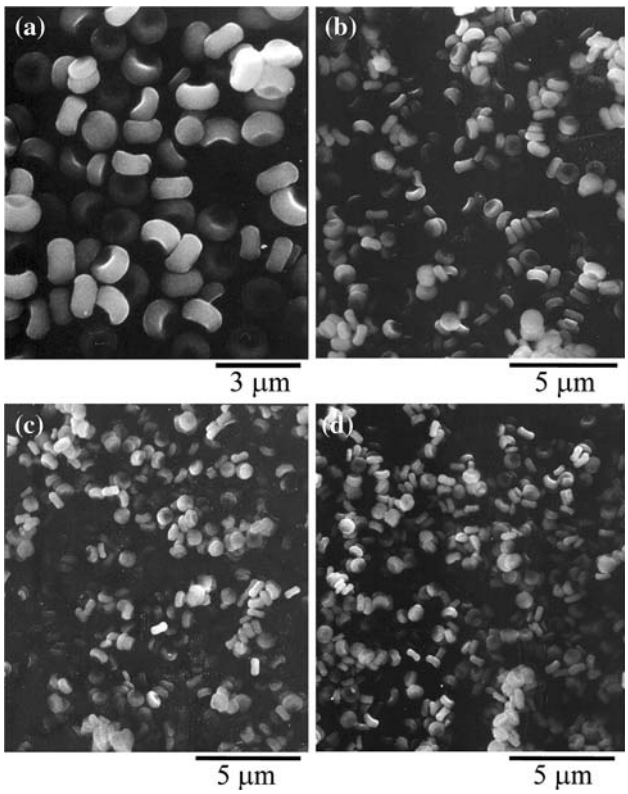

Fig. 3 SEM images of YBO_3: (**a**) as-synthesized product; (**b–d**) the product obtained by calcination at (**b**) 500 °C; (**c**) 800 °C; (**d**) 1,100 °C

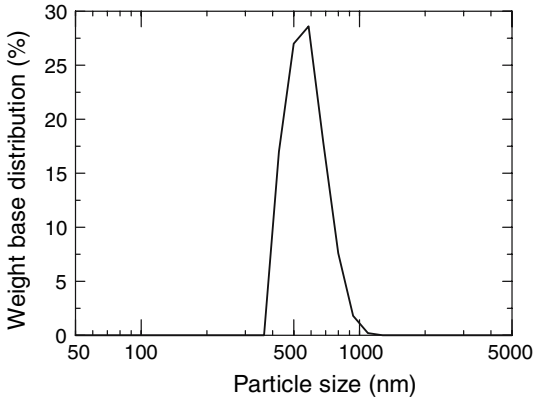

Fig. 4 Particle size distribution of as-synthesized YBO_3 measured by dynamic light scattering method

Table 2. The as-synthesized YBO_3 product had a surface area of 7 m^2/g, and the sample calcined at 500 °C had the surface area of 39 m^2/g, which was much larger than the hypothetical surface area (3 m^2/g) calculated assuming that each YBO_3 particle is spherical with a diameter of 1 μm (particle size), indicating that a pore system was developed in the particles by calcination. The N_2 adsorption isotherm of the sample calcined at 500 °C is shown in Fig. 8. A slight hysteresis was observed at a high relative-pressure region. The most significant point is that a large amount of N_2 molecules was adsorbed at the low relative-pressure region, $P/P_0 < 3.0 \times 10^{-2}$. This can be clearly seen by the *V–t* plot derived from the isotherm. When a sample has no pore systems, the plot gives a straight line going through the origin. When a sample has a micropore system, an abrupt decrease in the slope is observed. The *V–t* plot of the product clearly indicates the presence of micropores. The external surface area, that is the surface area after micropores are filled with the adsorbate molecules, was calculated from the slope of the second segment of the *V–t* plot to be 5 m^2/g, which was essentially identical with the value calculated assuming spherical particles. Therefore, the sample calcined at 500 °C had a large number of micropores. These pores seem to be originated from the combustion of organic residue filled in the deep crevices between the plate crystals. The BET surface area drastically decreased to the value calculated assuming spherical particles by calcination at 800 °C, indicating that the micropores of the sample calcined at 500 °C were closed by sintering of the crystallites (Fig. 9).

The crystallite size of the samples determined from the half-height widths of (110) and (104) diffraction peaks was approximately the same up to 800 °C. The crystallite size was much smaller than the particle size because of the presence of the deep crevices in the particles. However, calcination at 1,100 °C drastically decreased the crystallite sizes. This result is explained by the segregation of YBO_3 into B_2O_3 and Y_3BO_6, which was facilitated by evaporation of B_2O_3.

Synthesis of $REBO_3$ by the glycothermal reaction

The phases formed by the reaction of RE acetates and trimethoxyborane with RE/B = 1 for 2 h are summarized in Table 3. The $REBO_3$ phase was not obtained in the reaction of La acetate having a large RE ion size: only $La(OAc)_2(OH)$ [20] was obtained. Mixtures of RE(OAc)O, $REBO_3$ and the amorphous phase were obtained for Sm and Eu, and mixtures of $REBO_3$ and the amorphous phase were obtained for Gd–Er, while $REBO_3$ was formed as the sole product for Tm, Yb and Y (Fig. 10 and Table 3). It appears that RE acetate with small RE ion size easily reacted with borate ion in 1,4-BG: that is, the crystal growth in the reaction of RE acetate with small RE ion size proceeds faster than that with large ionic size. However, the reaction for Ho did not completely proceed and an amorphous product was also obtained in spite of the fact that the ionic size of Ho was almost the same with that of Y. In a previous paper, we found that the formation of $Y_3Al_5O_{12}$ by the glycothermal reaction of yttrium acetate

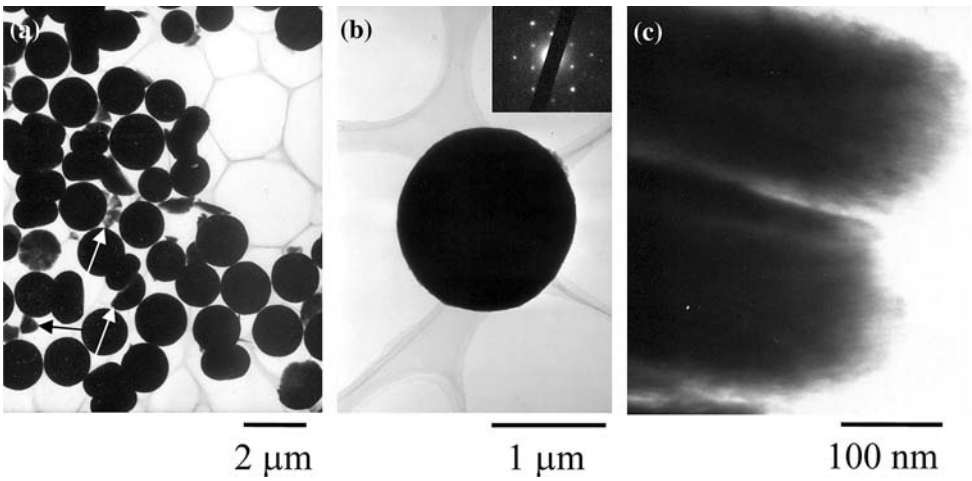

Fig. 5 TEM images of YBO_3 as synthesized by glycothermal reaction at 315 °C for 2 h. (**a**) Low magnification image; crushed particles are indicated by arrows. (**b**) Image of a particle and its electron diffraction pattern. (**c**) High magnification image the edge of YBO_3 particles whose *ab* planes are parallel to the electron beam

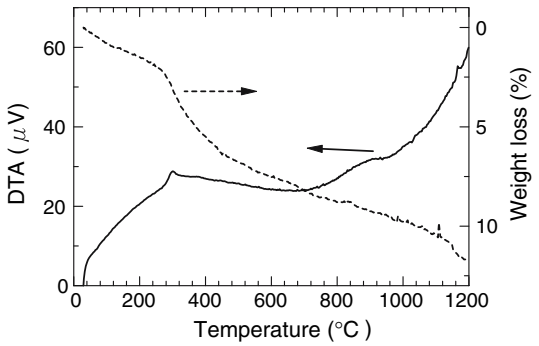

Fig. 6 TG-DTA of YBO_3 as synthesized by glycothermal reaction at 315 °C for 2 h

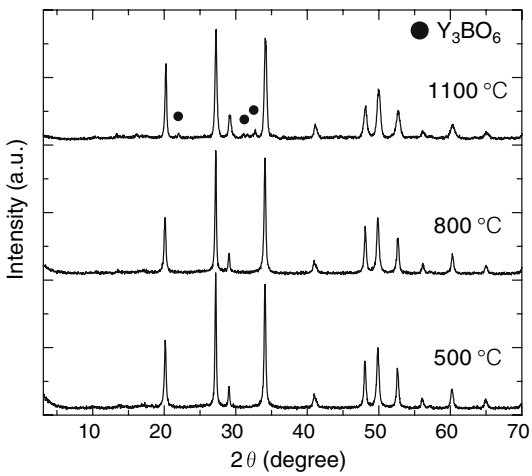

Fig. 7 XRD patterns of the samples obtained by calcination at various temperatures of YBO_3 synthesized by the glycothermal reaction

and alminum isopropoxide proceeded at 50 °C lower temperature than that required for the formation of $Ho_3Al_5O_{12}$. Therefore, there seems to be an unknown factor other than ionic radius governing the crystal growth or nucleation of Y compounds under the glycothermal conditions. Figure 11 and Tables 4 and 5 show the results for Rietveld analysis of the as-synthesized product obtained by the reaction of ytterbium acetate and trimethoxyborane. The product was comprised of two $YbBO_3$ phases with the $P6_3/m$ and $R\bar{3}c$ space groups [25]. The refinement led to residual values of $R_{wp} = 11.31\%$, $R_p = 8.01\%$, $R_e = 2.44\%$ and $S = 4.63$. The mass fractions of the $P6_3/m$ and $R\bar{3}c$ phases were 77 and 23%, respectively. The unit cell parameters for *a* and *c* axes of the $P6_3/m$ phase were 3.751 ± 0.002 and 8.790 ± 0.004 Å and those for *a* and *c* axes of the $R\bar{3}c$ phase were 4.933 ± 0.003 and 16.371 ± 0.007 Å, respectively. The calculated densities of the $P6_3/m$ and $R\bar{3}c$ phases were 7.19 and 6.69 g/cm^3, respectively, suggesting that the former phase has a higher thermodynamical stability than the latter phase. The $P6_3/m$ phase was obtained for Sm–Er and Y, while mixtures of the $P6_3/m$ and $R\bar{3}c$ phases were obtained for Tm and Yb.

The morphologies of the products obtained by prolonged reaction are shown in Fig. 12. The product obtained for Eu was composed of yarn-ball-like particles, but irregularly shaped particles were also observed. In the product for Ho, a large number of hexagonal plates were observed. The product obtained for Yb was composed of aggregates of disks and irregularly-shaped polyhedrons, the latter of which seems to be due to the $R\bar{3}c$ $REBO_3$ phase.

Prolonged reaction time increased the yield of $REBO_3$ with the $P6_3/m$ space group. Only $REBO_3$ was obtained for Eu–Yb and Y (Fig. 13 and Table 3). However, the reaction of La acetate and trimethoxyborane yielded $La(OAc)_2(OH)$ without formation of $LaBO_3$. The mixture of $P6_3/m$ and $R\bar{3}c$ were detected for Er and Tm, but for the Yb product, the peaks due to the $R\bar{3}c$ phase disappeared by prolonged reaction time, indicating that the phase transformed into the more stable $P6_3/m$ phase.

Table 2 Some properties of the as-synthesized product and the samples obtained by calcination

Sample	Phase	Crystallite size (nm)			BET surface area (m^2/g)
		(002)	(110)	(104)	
As-syn.	YBO_3	49	116	74	7
500 °C	YBO_3	49	88	74	39
800 °C	YBO_3	44	88	61	3
1,100 °C	YBO_3(87.5)[a] + Y_3BO_6(12.5)	52	35	30	3

[a] Mass fractions (%) of YBO_3 and Y_3BO_6 phases calculated by Rietveld analysis; the refiment led to residual values of R_{wp} = 7.43%, R_p = 5.44%, R_e = 4.73% and S = 1.57

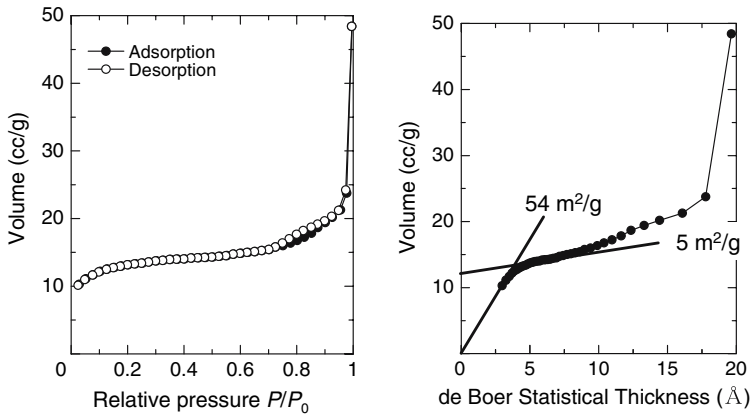

Fig. 8 N_2 adsorption isotherm (left) and V–t plot (right) derived from the adsorption branch of the isotherm of the sample obtained by 500 °C calcination of YBO_3

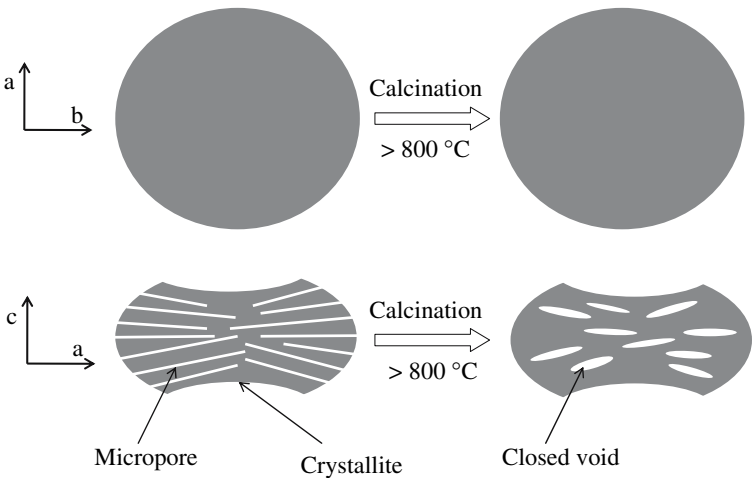

Fig. 9 Cartoon for the change in pore structure by calcination

Table 3 Phase formed by reaction of rare earth acetate and trimethoxyborane at 315 °C[a,b]

Reaction time (h)	La	Nd	Sm	Eu	Gd	Tb	Dy, Ho	Er	Tm	Yb	Y
2	$La(OAc)_2(OH)$	–	P, A, Ac	P, A, Ac	P, A	A	P, A	P, A	P, R, U	P, R	P
6	$La(OAc)_2(OH)$	P, A, Ac	P, A	P	P	P	P	P, R	P, R, U	P, U	P

[a] Phase determined by XRD

[b] P, $REBO_3$ with $P6_3/m$ space group; R, $REBO_3$ with $R\bar{3}c$ space group; A, amorphous; Ac, RE(OAc)O; U, unknown phase

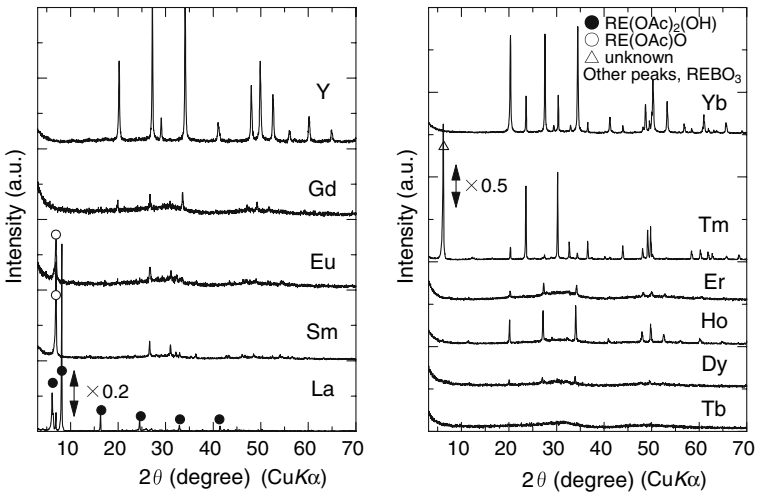

Fig. 10 XRD patterns of the products as synthesized by the glycothermal reaction of RE acetates and trimethoxyborane with RE/B = 1 in 1,4-BG at 315 °C for 2 h

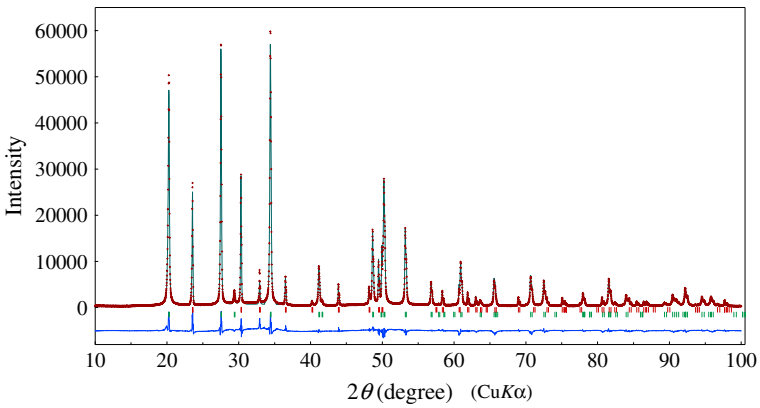

Fig. 11 Observed, calculated, and difference patterns obtained by Rietveld analysis of $YbBO_3$ as synthesized by glycothermal reaction at 315 °C for 2 h

Table 4 Crystallographic data of $YbBO_3$ obtained by glycothermal method

Element	Site	g^a	Atomic coordinates			B^b
			x	y	z	
Oa	4*f*	1	0.667	0.333	0.095 ± 0.001	1.0
Ob	6*h*	1/3	0.850 ± 0.017	−0.214 ± 0.006	0.250	1.0
B	6*h*	1/3	0.584 ± 0.262	0.417 ± 0.262	0.250	1.5
Yb	2*b*	1	0	0	0	0.4

Space group $P6_3/m$ (No. 176)

[a] Site occupacy

[b] Isotropic displacement parameter

Table 5 Crystallographic data of $YbBO_3$ obtained by glycothermal method

Element	Site	g^a	Atomic coordinates			B^b
			x	y	z	
O	18*e*	1	0.697 ± 0.002	0	0.250	1.0
B	6*a*	1	0	0	0.250	1.5
Yb	6*b*	1	0	0	0	0.4

Space group $R\bar{3}c$ (No. 167)

[a] Site occupacy

[b] Isotropic displacement parameter

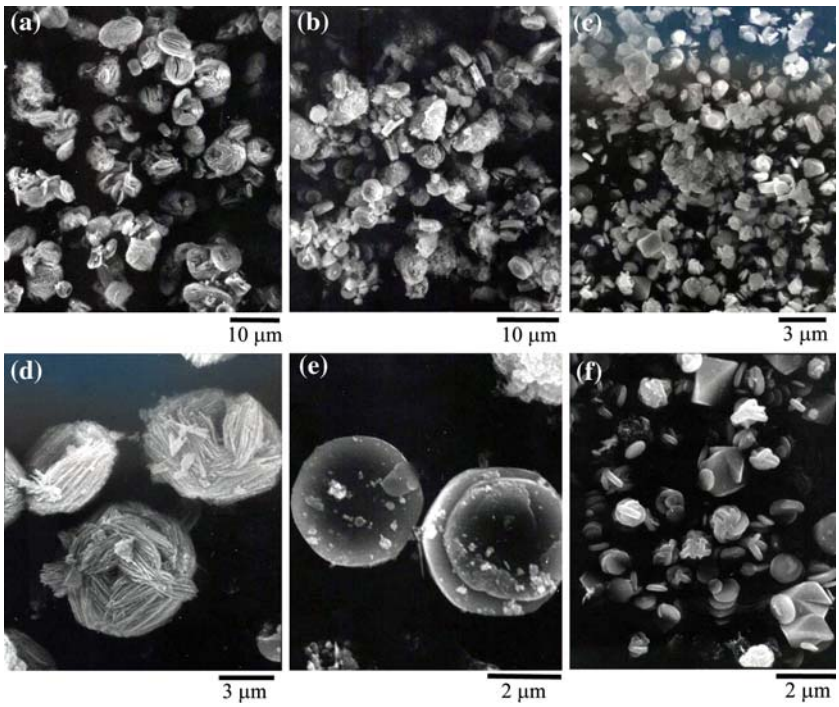

Fig. 12 SEM image of $REBO_3$ as synthesized by glycothermal reaction at 315 °C for 2 h: (**a**, **d**), Eu; (**b**, **e**), Ho; (**c**, **f**), Yb

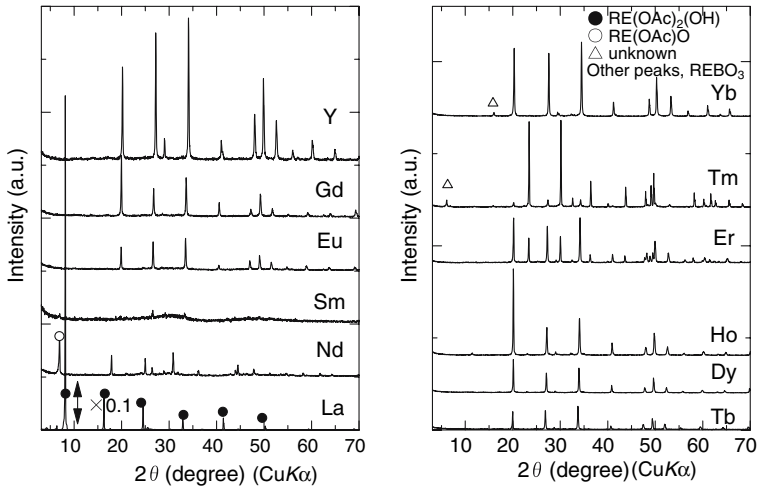

Fig. 13 XRD patterns of the products as synthesized by the glycothermal reaction of RE acetates and trimethoxyborane with RE/B = 1 in 1,4-BG at 315 °C for 6 h

The morphologies of the products obtained by prolonged reaction are shown in Fig. 14. The products obtained for Eu, Ho and Y were composed of spheroidal particles with hexagonal-pyramidal craters at the both sides. Small irregularly shaped particles were also observed for the Eu product, and hexagonal plates were also observed in the Ho product. The particle size of the Y product was 3 μm, which was much larger than that obtained by the reaction for 2 h. Enlargement of the particle size with the prolonged reaction indicates that Ostwald ripening took place during the glycothermal treatment. The Yb product was composed of aggregates of hexagonal plate particles.

In a previous paper, the mechanisms for the crystallization of rare earth gallium garnet [17] in glycothermal reaction were discussed. Based on the arguments, the following scheme is proposed for the formation of $REBO_3$: the important step for the glycothermal reaction is the heterolytic cleavage of the C–O bond of $HO(CH_2)_n$–O–B< formed by the alkoxyl exchange reaction between trimethoxyborane and glycol; when 1,4-BG (n = 4) was used, the cleavage of the C–O bond in $HO(CH_2)_n$–O–B< was facilitated by participation of the intramolecular hydroxyl group. The O^- anion formed by the heterolytic cleavage of the C–O bond reacts with RE^{3+} ion, and the RE–O–B bond

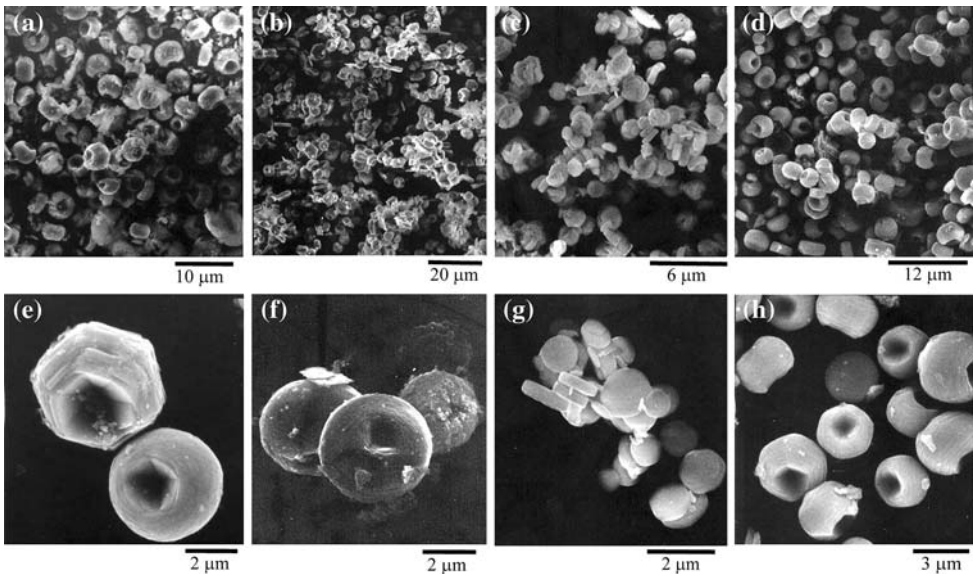

Fig. 14 SEM image of $REBO_3$ as synthesized by glycothermal reaction at 315 °C for 6 h: (**a**, **e**) Eu; (**b**, **f**) Ho; (**c**, **g**) Yb; (**d**, **h**) Y

is formed. In the present reaction, RE–O–B was not formed for large RE ions with lower Coulomb force.

Mono-dispersed particles can be prepared if a burst of nucleation takes place at the early stage of the reaction and if nucleation does not take place during the crystal growth stage. In the present reaction, nucleation occurs at a high concentration level of reactants in solution, which is supersaturated with respect to $REBO_3$. Once nucleation occurs, the concentration level decreases, which is determined by the balance between the dissolution rate and the consumption rate of the reactants in the solution by the crystal growth. When crystals grow rapidly, the concentration of the reactants becomes low, and nucleation does not take place during the crystal growth stage. The reaction for Y was completed within 2 h, while for Eu or Ho the reaction was not completed in 2 h resulting in formation of amorphous products. This result suggests that the crystal growth in the reaction of Eu or Ho is slower than that in the reaction of Y. The nucleation takes place during the crystal growth stage of $EuBO_3$ or $HoBO_3$. Therefore, the particle size of the Eu and Ho products were distributed widely. On the other hand, rapid crystal growth of YBO_3 decreases the concentration of the reactant in the solution, thus facilitating the formation of mono-dispersed particles.

Conclusions

The reaction of yttrium acetate and trimethoxyborane at 315 °C for 2 h directly yielded phase-pure YBO_3. The YBO_3 particles were spheroidal with a diameter of 1 μm and, the selected area electron diffraction of a whole particle exhibited a single crystal pattern. Each particle was grown from one nucleus, but was divided into smaller crystallites by the crevices.

The glycothermal reaction of RE acetates with trimethoxyborane at 315 °C for 2 h yielded $REBO_3$ crystals with $P6_3/m$ and $R\bar{3}c$ for Tm and Yb, while the space group of the $REBO_3$ crystal obtained from Sm–Er and Y was $P6_3/m$. The YBO_3 products were composed with spheroidal particles with hexagonal-pyramidal craters at the both sides, and the morphologies such as yarn-ball-like particles, hexagonal plates, disks or polyhedrons were also observed depending on the RE element. Prolonged reaction time (6 h) yielded $REBO_3$ without contamination of the amorphous product or RE(OAc)O for Eu–Yb, and Y. The space group of $YbBO_3$ obtained by prolonged reaction time was $P6_3/m$, indicating that transformation of the $R\bar{3}c$ phase into the $P6_3/m$ phase took place during the reaction.

References

1. Ronda CR, Jüstel T, Nikol H (1998) J Alloys Compd 275–277:669
2. Li Z, Zeng J, Chen C, Li Y (2006) J Cryst Growth 286:487
3. Lemanceau S, Bertrand-Chadeyron G, Mahiou R, El-Ghozzi M, Cousseins JC, Conflant P, Vannier RN, (1999) J Solid State Chem 148:229
4. Kim KN, Jung H-K, Park HD, Kim D (2002) J Mater Res 17:907
5. Tukia M, Hölsä J, Lastusaari M, Niittykoski J (2005) Opt Mater 27:1516
6. Kim D-S, Lee R-Y (2000) J Mater Sci 35:4777
7. Boyer D, Bertrand-Chadeyron G, Mahiou R, Lou L, Brioude A, Mugnier J (2001) Opt Mater 16:21
8. Boyer D, Bertrand-Chadeyron G, Mahiou R, Caperaa C, Cousseins J-C (1999) J Mater Chem 9:211
9. Wei Z, Sun L, Liao C, Yin J, Jiang X, Yan C, Lü S (2002) J Phys Chem B 106:10610
10. Wei Z-G, Sun L-D, Liao C-S, Jiang X-C, Yan C-H (2002) J Mater Chem 12:3665
11. Jiang X-C, Sun L-D, Feng W, Yan C-H (2004) Cryst Growth Des 4:517
12. Kim T, Kang S (2005) Mater Res Bull 40:1945

13. Jiang X-C, Yan C-H, Sun L-D, Wei Z-G, Liao C-S (2003) J Solid State Chem 175:245
14. Jiang X-C, Sun L-D, Yan C-H (2004) J Phys Chem B 108:3387
15. Zhang J, Lin J (2004) J Cryst Growth 271:207
16. Inoue M, Otsu H, Kominami H, Inui T (1995) J Alloys Compd 226:146
17. Inoue M, Nishikawa T, Otsu H, Kominami H, Inui T (1998) J Am Ceram Soc 81:1173
18. Inoue M (2005) Solvothermal Synthesis, In: Lee B, Komarneni S (eds) Chemical processing of ceramics, 2nd edn., Chap. 2. Taylor & Francis, Boca Raton, FL
19. Izumi F, Ikeda T (2000) Mater Sci Forum 321–324:198
20. Inoue M, Nishikawa T, Kominami H, Inui T (2000) J Mater Sci 35:1541
21. Boyer D, Bertrand-Chadeyron G, Mahiou R, Brioude A, Mugnier J (2003) Opt Mater 24:35
22. Lin JH, Zhou S, Yang LQ, Yao GQ, Su MZ, You LP, (1997) J Solid State Chem 134:158
23. Chadeyron G, El-Ghozzi M, Mahiou R, Arbus A, Cousseins JC (1997) J Solid State Chem 128:261
24. Nakamura A, Nambu N, Saitoh H (2005) Sci Technol Adv Mater 6:210
25. Cox JR, Keszler DA (1994) Acta Cryst C50:1857